ELSEVIER

# Stabilization of nucleic acid triplexes by high concentrations of sodium and ammonium salts follows the Hofmeister series[1]☆

Laurence Lavelle[a,b,]*, Jacques R. Fresco[a,]*

[a]*Department of Molecular Biology, Princeton University, Princeton, NJ 08544, USA*
[b]*Department of Chemistry and Biochemistry, University of California Los Angeles, Los Angeles, CA 90095, USA*

## Abstract

The thermal stability of the triplexes $d(C^+-T)_6 \vdots d(A-G)_6 \bullet d(C-T)_6$ and $d(T)_{21} \vdots d(A)_{21} \bullet d(T)_{21}$ was studied in the presence of high concentrations of the anions $Cl^-$, $HPO_4^{2-}$, $CH_3COO^-$, $SO_4^{2-}$ and $ClO_4^-$. Thermally-induced triplex and duplex transitions were identified by UV- and CD-spectroscopy and $T_m$ values were determined from melting profiles. A thermodynamic analysis of triplex transitions shows the limitations of commonly used treatments for determining the associated release or uptake of salt, solute or water. Enhancement of the stability of these triplexes follows the rank order of the Hofmeister series for anions of sodium and ammonium salts, whereas water structure-breaking solutes have the opposite effect. The rank order for the Hofmeister series $ClO_4^- < I^- < Br^- < Cl^- < HPO_4^{2-} < SO_4^{2-}$ is shown to follow their effective surface charge densities.
© 2003 Elsevier Science B.V. All rights reserved.

*Keywords:* Triplex stabilization; Hofmeister anion series

## 1. Introduction

In view of their polyanionic strands, it is natural for the stability of nucleic acid triplexes to be especially dependent on the concentration and type of cation in solution. While stabilization by cations is a general consequence of the shielding of the high negative charge density of the three phosphodiester backbones, the chemical nature of a cation can otherwise affect its interaction with nucleic acids when it is present at high concentrations, particularly by affecting water structure and its interaction with the macromolecule. The triplex stabilizing effect of group 1, (e.g. $Na^+$, $K^+$) and group 2 (e.g. $Mg^{2+}$), cations has been extensively characterized, e.g. [1]; so has the stabilization by the organic polyamines, spermine and spermidine, which are positively charged at neutral pH, e.g. [2].

To date, however, there has been no systematic exploration of the wider range of solution additives that affect the stability of triplexes. Such an analysis has the potential to provide insights into the factors that determine the stability of triplexes and the mechanism of their formation. In the present work, the effect of high concentrations of the sodium and ammonium salts of $Cl^-$, $HPO_4^{2-}$, $CH_3COO^-$, $SO_4^{2-}$ and $ClO_4^-$ on the stability of the triplexes $d(C^+\text{-}T)_6\text{:}d(A\text{-}G)_6\bullet d(C\text{-}T)_6$ and $d(T)_{21}\text{:}d(A)_{21}\bullet d(T)_{21}$ was determined. It was the aim of this study to distinguish the effect of the cations on the negatively charged nucleic acid backbone from any effect the anions might have by altering the chemical potential and structure of the aqueous solvent.

## 2. Materials and methods

### 2.1. Deoxyoligomers

$d(A\text{-}G)_6$ and $d(C\text{-}T)_6$ were synthesized, purified and analyzed as previously [3]. Molar extinction coefficients determined after phosphodiesterase I digestion, $\lambda_{260} = 9890$ for $d(A\text{-}G)_6$ and $\lambda_{260} = 8510$ for $d(C\text{-}T)_6$ at 25 °C in $2.6 \times 10^{-5}$ M Tris pH 7.4/ $2.4 \times 10^{-5}$ M $MgCl_2$, were used to determine oligomer concentration. $d(T)_{21}$ and $d(A)_{21}$ were similarly synthesized and purified (Midland Certified Reagent Co., Midland, Texas) and analyzed for purity. The concentrations of these strands in $ddH_2O$ were calculated using the molar extinction coefficients at 25 °C for poly (dA) ($\lambda_{257} = 8600$) and poly(dT) ($\lambda_{265} = 8700$).

### 2.2. Sample preparation

Unless otherwise stated, triplexes were prepared in a *mixing buffer* (MB) of 0.15 M NaCl/0.005 M $MgCl_2$/0.01 M cacodylate, titrated to the desired pH ($\pm 0.1$). Thermal stability of triplexes and duplexes was compared with reference to their stability in MB at pH 7.0. Triplex mixtures were made with equimolar stocks of the two strands; after forming the duplex, a stoichiometric amount of the third strand was added. All samples were made with $ddH_2O$, buffered with 0.01 M cacody-

late, and titrated to the desired pH. Where checked, the pH after a melting profile was unchanged.

### 2.3. UV spectroscopy and melting profiles

Absorption spectra and thermal melting profiles were determined in a computer-driven AVIV 14DS spectrophotometer equipped with a thermoelectrically-controlled cell holder for cells of 1 cm pathlength. Filtered dry air was passed through the cell compartment to prevent condensation on the cell walls at low temperatures. The flow rate was set low enough to avoid a temperature gradient between the sample and the cell holder. This avoidance was confirmed by monitoring the temperature in the sample and cell holder in preliminary trials. Briefly summarizing, melting profiles were obtained by measuring absorbance every nm between 230–290 nm and every 1 °C over the desired temperature range. Duplicate *equilibrium* melting profiles were obtained by recording scans only after the sample reached the set temperature (8 min), as confirmed by the absence of further absorbance change on longer incubation. These spectra were used to obtain profiles at appropriate wavelengths, from which equilibrium transition
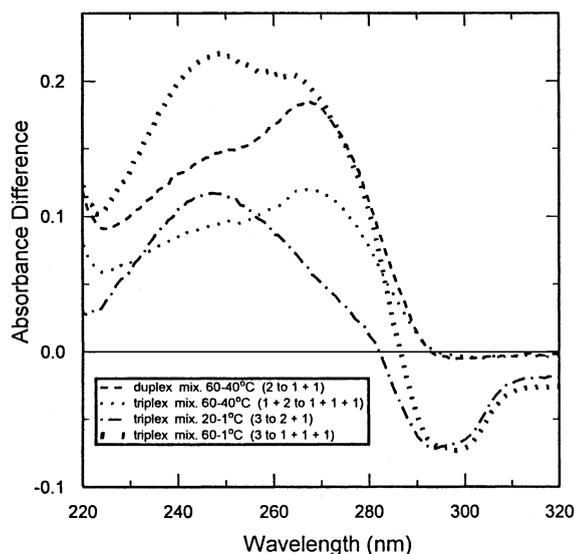


Fig. 1. Difference spectra for $d(C^+\text{-}T)_6\text{:}d(A\text{-}G)_6\bullet d(C\text{-}T)_6$ and $d(A\text{-}G)_6\bullet d(C\text{-}T)_6$ in MB at pH 7.0.

temperatures, $T_m$ values, ($\pm 0.5$ °C) were determined from the midpoint of the transition. Previously, it was established that melting profiles obtained by the method described correspond to the more difficult to measure cooling profiles. Unless otherwise stated, values for $T_m$ and percent hypochromicity were obtained from profiles at 260 nm. All UV-melting profiles, spectra and difference spectra were measured against a solvent blank, but were not corrected for dilution due to thermal expansion, which is small over the temperature range of a cooperative transition. For triplexes, percent hypochromicity was calculated using $\{[A_{260}(\text{duplex}+\text{coil})\text{-}A_{260}(\text{triplex})]/A_{260}(\text{duplex}+\text{coil})\}\times 100$ for $3\rightarrow 2+1$ transitions, and $\{[A_{260}(\text{coil})\text{-}A_{260}(\text{triplex})]/A_{260}(\text{coil})\}\times 100$ for $3\rightarrow 1+1+1$ transitions. Because of their UV absorbance, bromide, iodide and thiocyanide salts could not be investigated.

## 2.4. CD spectroscopy

CD was measured every 0.2 nm (1 s. average, with a 1.5 nm bandwidth) from 320 to 200 nm at 1 °C on a computer-driven AVIV 62DS spectrometer with a thermoelectrically-controlled cell holder. The cell compartment was continuously purged with dry $N_2$. The spectral data was smoothed by a least-squares polynomial fit of the 6th order.

## 3. Results

### 3.1. Spectral identification of the triplexes

The melting of triplexes is often characterized by the presence of two transitions in the UV-melting profile (e.g. Fig. 2a, Fig. 4), the first transition reflecting the release of third strand from the core duplex, and the second, at a higher
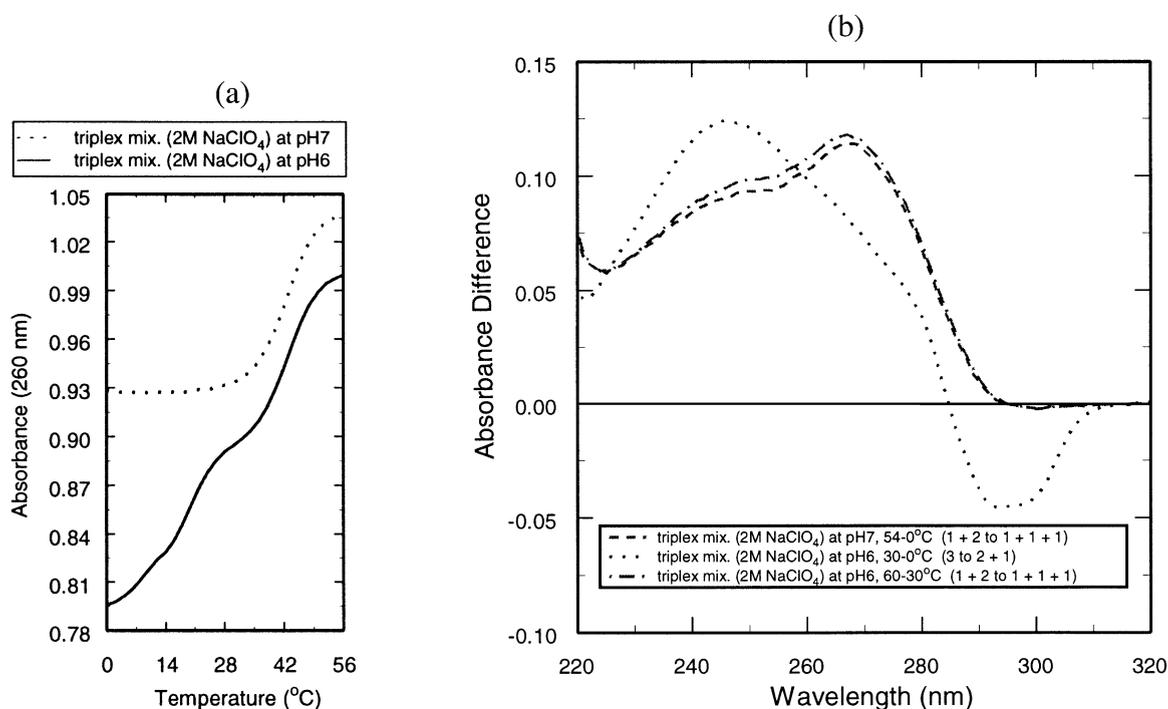


Fig. 2. (a) UV melting profiles for the triplex mixture d(C$^+$-T)$_6$+d(A-G)$_6$•d(C-T)$_6$ in 2.0 M NaClO$_4$ at pH 7.0 and 6.0. At pH 7.0 the profile corresponds to that for the core duplex d(A-G)$_6$•d(C-T)$_6$. (b) Difference UV spectra for the triplex mixture at pH 7.0 between 54 and 0 °C and at pH 6.0 between 30 and 0 °C and between 60 and 30 °C.

temperature, resulting from the dissociation of the core duplex [4]. However, triplex melting, particularly at high ionic strength, can lead directly to single strands [1]. Moreover, sometimes a biphasic melting profile can be misleading, the low temperature transition being due not to the dissociation of a putative third strand from a core duplex, but merely to a self-structure formed by the putative third strand as an alternative to triplex formation. To avoid such possible misleading observations, UV difference spectra and CD spectra were also used to establish triplex formation.

### 3.2. $d(C^+-T)_6 \cdot d(A-G)_6 \cdot d(C-T)_6$

The UV-spectroscopic characterization of this triplex, in particular its unique difference spectrum on dissociation of the third strand from the core duplex above pH 4.6, has been described in detail [3]. Fig. 1 shows all the possible difference spectra in mixing buffer (MB) at pH 7.0:

1. Difference spectrum for the dissociation of the duplex in a duplex mixture; 60 °C spectrum (single strands) $-40$ °C spectrum (duplex), giving the difference spectrum for a $2 \rightarrow 1+1$ transition.

2. Difference spectrum for the dissociation of the duplex in a triplex mixture; 60 °C spectrum (single strands) $-40$ °C spectrum (duplex + single strand), giving the difference spectrum for a $1+2 \rightarrow 1+1+1$ transition. The difference spectrum for dissociation of the duplex contains a major peak with $\lambda_{max}=270$ nm and a slightly lower intensity peak with $\lambda_{max}=250$ nm.

3. Difference spectrum for the dissociation of the third strand from the core duplex; 20 °C spectrum (single strand + duplex) $-1$ °C spectrum (triplex), giving the difference spectrum for a $3 \rightarrow 2+1$ transition. This difference spectrum has a peak with $\lambda_{max}=245$ nm and a trough with $\lambda_{min}=295$ nm.

4. Difference spectrum for the direct dissociation of the triplex to its three strands; 60 °C spectrum (single strands) $-1$ °C spectrum (triplex), giving the difference spectrum for a $3 \rightarrow 1+1+1$ transition. This difference spectrum has the characteristics of both third strand dissociation from duplex and duplex dissociation to single strands, with peaks at $\sim 247$ and $\sim 267$ nm and a trough at 295 nm.

For this triplex, these unique spectral characteristics for dissociation of the third strand and of the duplex, evident in the difference spectra in Figs. 1 and 2, enabled unambiguous identification of the transitions observed in the various UV-melting profiles. In addition, the identity of many triplex transitions was confirmed by lowering the pH and observing an increase in triplex stability with no concommitant increase in duplex stability.

As an illustration of this approach, we consider the melting profiles of the triplex mixture $d(C^+-T)_6 + d(A-G)_6 \cdot d(C-T)_6$ in 2.0 M NaClO$_4$ at pH 7.0 and 6.0. Fig. 2a shows a single transition with a $T_m$ of 42 °C at neutrality, but a profile with a biphasic transition with $T_m$ values of 18° and 43 °C at pH 6.0. In Fig. 2b, the difference spectrum at pH 7.0 confirms that the single transition represents dissociation of duplex only. At pH 6.0, the difference spectrum for the first transition clearly shows that it involves third strand release $(3 \rightarrow 2+1)$, while that for the second transition is so similar to those at pH 7.0 and for the duplex mixture in MB at pH 7.0 (Fig. 1, plot 1), as to identify it with the melting of the core duplex.
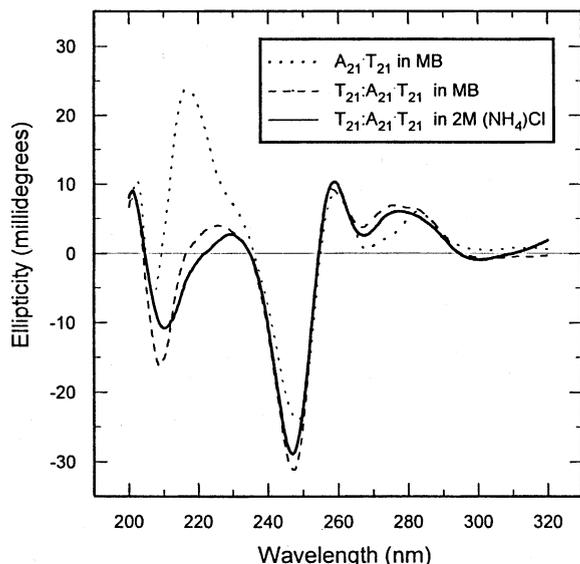


Fig. 3. CD-spectra at 1 °C of $d(A)_{21} \cdot d(T)_{21}$ and $d(T)_{21} : d(A)_{21} \cdot d(T)_{21}$ in MB at pH 7.0 and of $d(T)_{21} : d(A)_{21} \cdot d(T)_{21}$ in 2.0 M (NH$_4$)Cl at pH 7.0.

Table 1
$T_m$ values for $d(T)_{21} \cdot d(A)_{21} \cdot d(T)_{21}$ in various salts[2]

| Conditions[d] | 1st Transition | | 2nd Transition | |
|---|---|---|---|---|
| | $T_m$ °C | Hypochromicity % | $T_m$ °C | Hypochromicity % |
| **MB-pH 7.0** | **23** | **18** | **53** | **15** |
| 0.4 M NaCl-pH 7.0 | 24 | 17 | 58 | 19 |
| 0.8 M | 42 | 18 | 62 | 17 |
| 1.0 M | 49[a] | 18 | 64[a] | 18 |
| 2.0 M | 66[b] | 33 | – | – |
| 3.0 M | 70[b] | 33 | – | – |
| 5.0 M | 72[b] | 33 | – | – |
| 2.0 M $Na_2HPO_4$-pH 7.0 | 80[b] | 33 | – | – |
| 2.0 M $NaOOCCH_3$-pH 7.0 | 66[b] | 33 | – | – |
| 2.0 M $Na_2SO_4$-pH 7.0 | 80[b] | 33 | – | – |
| 2.0 M $NaClO_4$-pH 7.0 | 44[b] | 30 | – | – |
| 1.0 M $NH_4Cl$-pH 7.0 | 65[b] | 36 | – | – |
| 2.0 M | 71[b] | 36 | – | – |
| 3.0 M | 76[b] | 36 | – | – |
| 1.0 M $(NH_4)_2SO_4$-pH 7.0 | 71[b] | 36 | – | – |
| 2.0 M | 83[b] | 36 | – | – |
| 3.0 M | 93[b] | 36[c] | – | – |

[a] Overlapping transitions.

[b] $3 \rightarrow 1$ transition.

[c] Obtained by extrapolation.

[d] 0.01 M cacodylate pH 7.0. Salt concentrations are given as the molarity of the anion.

## 3.3. $d(T)_{21} \cdot d(A)_{21} \cdot d(T)_{21}$

For this triplex, the UV-difference spectrum for release of the third strand from the core duplex $d(A)_{21} \cdot d(T)_{21}$ is similar to that for dissociation of the core duplex. Hence, these difference spectra are not the most sensitive criteria for distinguishing triplex from duplex. However, the CD-spectra of the triplex and duplex are substantially different, allowing for more confident characterization of the contents of triplex mixtures under different conditions. Hence, the transitions obtained from the UV-melting profiles of mixtures with these strands were characterized as reflecting triplex or duplex melting based upon the number of transitions observed, the percent hypochromicity, and the CD spectrum at each plateau in the profiles.

Fig. 3 shows the CD spectra of the duplex and triplex mixtures in MB. The duplex spectrum gives an intense band with $\lambda_{max}$ at 217 nm and an intense band with $\lambda_{min}$ at 247 nm. Between 235 and 320 nm the triplex has a spectrum similar to that of the

duplex, but below 235 nm it has an additional $\lambda_{min}$ at 209 nm. The CD spectra for the triplex $d(T)_{21} \cdot d(A)_{21} \cdot d(T)_{21}$ and the duplex $d(A)_{21} \cdot d(T)_{21}$ are similar to those in the literature for poly $d(T) \cdot d(A) \cdot d(T)$ and poly $d(A) \cdot d(T)$ [5].

The CD-spectrum of $d(T)_{21} \cdot d(A)_{21} \cdot d(T)_{21}$ in 2.0 M $(NH_4)Cl$ (Fig. 3) is clearly that of the triplex. Hence, the single transition with $T_m = 71$ °C, and 36% hypochromicity (Table 1) in the UV melting

[2] In order to facilitate comparison with literature $T_m$ values at neutrality, and the fact that triplexes containing dC or rC residues show pH-dependent stability, triplex stability was determined at pH 7.0. In the case of our 2.0 M phosphate solutions (4.0 M $Na^+$) at pH 7.0, the phosphate di-anion is possibly present at a lower concentration since the second $pK_a = 7.2$ between $\sim 0.01$ and 0.1 M phosphate [29]. However, this is difficult to quantify as the $pK_a$ value for a 2.0 M phosphate solution has not been determined. In fact, since the second $pK_a$ for phosphoric acid is slightly lowered with increasing temperature, and more so with increasing sodium phosphate concentration [30], it is possible that at pH 7.0 only the phosphate di-anion is present at the very high sodium phosphate concentrations where the triplex $T_m$ values have been measured.
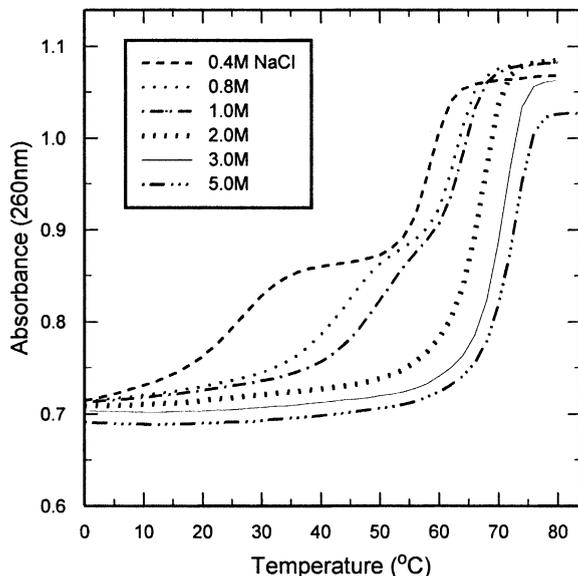
Fig. 4. UV melting profiles at 260 nm for $d(T)_{21}$:$d(A)_{21}$•$d(T)_{21}$ at various NaCl concentrations at pH 7.0.

profile of the triplex mixture in that solvent (see comparable profile in NaCl, Fig. 4) represents $3 \rightarrow 1+1+1$ melting, with the hypochromic change corresponding to the sum of the changes for the $3 \rightarrow 2+1$ and the $2 \rightarrow 1+1$ transitions.

## 3.4. Variation in triplex stability with the anion

Tables 1 and 2 list the $T_m$ values and the percent hypochromicity obtained from the UV-melting profiles at 260 nm of $d(T)_{21}$:$d(A)_{21}$•$d(T)_{21}$ and $d(C^+-T)_6$:$d(A-G)_6$•$d(C-T)_6$.

Fig. 4 shows how the course of melting of $d(T)_{21}$:$d(A)_{21}$•$d(T)_{21}$ is affected by NaCl concentration. Below 2.0 M, melting is biphasic, whereas at NaCl $\geq 2.0$ M, it is monophasic. The qualitative effect of NaCl concentration on the pathway of melting of this triplex is essentially the same as it is for the melting of poly r(U:A•U), although the salt concentration at which melting changes from biphasic to monophasic occurs near 0.2 M Na$^+$ for poly r(U:A•U) [1].

The data in Table 1 show that relative to NaCl, the salts Na$_2$HPO$_4$, Na$_2$SO$_4$, (NH$_4$)Cl and (NH$_4$)$_2$SO$_4$ all enhance the stability of $d(T)_{21}$:$d(A)_{21}$•$d(T)_{21}$, whereas NaClO$_4$ destabilizes this triplex. Interestingly, $T_m$ for this triplex is the same in 2.0 M NaOOCCH$_3$ and NaCl (Table 1). The semilog plot of $T_m$ vs. *anion* concentration in Fig. 5 together with the hypochromicity data in Table 1 show that both NH$_4$Cl and (NH$_4$)$_2$SO$_4$ induce $3 \rightarrow 1$ melting of $d(T)_{21}$:$d(A)_{21}$•$d(T)_{21}$ at least by 1.0 M anion, and that both these salts are better stabilizers of this triplex than NaCl. The enhancement by NH$_4$Cl must mean that NH$_4^+$ is more effective than Na$^+$ in this regard. At the same time, the *apparently* greater enhancement *by the same anion concentration* of (NH$_4$)$_2$SO$_4$ than NH$_4$Cl could be due to more than the difference in anion, since the sulfate salt has twice as much ammonium ion as the chloride salt.

The triplex $d(C^+-T)_6$:$d(A-G)_6$•$d(C-T)_6$ differs from $d(T)_{21}$:$d(A)_{21}$•$d(T)_{21}$ in its requirement for protonated third strand C residues [3]. One consequence is that there is no concentration of any salt at which the triplex is more stable than the core duplex; hence, this triplex always melts by a $3 \rightarrow 2+1$ transition, i.e. by dissociating the third strand, leaving core duplex (Table 2), rather than by melting directly to single strands. Previously [3], the destabilization of $d(C^+-T)$:$d(A-G)_6$•$d(C-T)_6$ at NaCl$>$ 0.8 M (Fig. 6) has been attributed to the effect of high ionic strength on the p$K_a$ of the third strand C residues. It is curious that such destabilization is not seen with Na$_2$HPO$_4$, NaOOCH$_3$, Na$_2$SO$_4$ and (NH$_4$)$_2$SO$_4$ (Fig. 6). Instead, these salts, in the order listed, increasingly stabilize this triplex more effectively than NaCl, whereas NaClO$_4$ and NH$_4$Cl destabilize it (Table 2). However, this stabilization is not enough to promote $3 \rightarrow 1$ melting, i.e. to raise the stability of the triplex to that of the core duplex. Perhaps, the lack of triplex destabilization by high concentrations of these salts is due to the more effective stabilization by their anions relative to Cl$^-$ (see below), which masks the general ionic strength effect on the p$K_a$ of C. It is also worthy of note that NaClO$_4$ is the only salt that also destabilizes the duplex.

Table 2
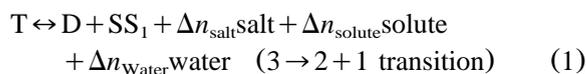$T_m$ values for d(C$^+$-T)$_6$:d(A-G)$_6$•d(C-T)$_6$ in various salts

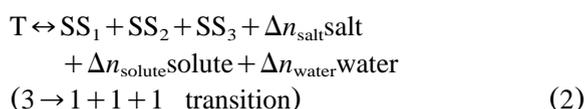| Conditions[b] | 1st Transition | | 2nd Transition | |
|---|---|---|---|---|
| | $T_m$ °C | Hypochromicity % | $T_m$ °C | Hypochromicity % |
| MB-pH 5.0 | 29 | 12 | 50 | 9 |
| **MB-pH 7.0** | **11** | **12** | **50** | **10** |
| MB-pH 7.5 | 1 | 4 | 50 | 10 |
| 0.4 M NaCl-pH 7.0 | 7 | 7 | 53 | 12 |
| 0.5 M | 8 | 14 | 54 | 10 |
| 0.8 M | 10 | 16 | 56 | 11 |
| 0.9 M | 10 | 17 | 56 | 11 |
| 1.0 M | 9 | 17 | 54 | 12 |
| 2.0 M | 7 | 13 | 54 | 12 |
| 3.0 M | 5 | 2 | 57 | 7 |
| 5.0 M | – | – | 51 | 10 |
| 0.4 M Na$_2$HPO$_4$-pH 7.0 | 8 | 9 | 54 | 12 |
| 0.8 M | 12 | 11 | 56 | 11 |
| 2.0 M | 15 | 11 | 57 | 11 |
| 2.0 M-pH 6.5 | 29 | 14 | 59 | 11 |
| 0.4 M NaOOCCH$_3$-pH 7.0 | 9 | 12 | 53 | 11 |
| 0.8 M | 12 | 12 | 56 | 11 |
| 2.0 M | 15 | 13 | 55 | 11 |
| 3.0 M | 16 | 13 | 54 | 12 |
| 0.4 M Na$_2$SO$_4$-pH 7.0 | 14 | 12 | 54 | 10 |
| 0.8 M | 17 | 13 | 55 | 12 |
| 2.0 M | 21 | 14 | 58 | 11 |
| 0.8 M-pH 7.2 | 9 | 8 | 56 | 11 |
| 2.0 M NaClO$_4$-pH 7.0 | – | – | 42 | 11 |
| 2.0 M-pH 6.0 | 18 | 12 | 43 | 10 |
| 0.4 M NH$_4$Cl-pH 7.0 | 8 | 5 | 56 | 12 |
| 0.8 M | – | – | 54 | 12 |
| 2.0 M | – | – | 58 | 12 |
| 0.4 M (NH$_4$)$_2$SO$_4$-pH 7.0 | 8 | 4 | 55 | 12 |
| 0.8 M | 19 | 13 | 57 | 12 |
| 2.0 M | 28 | 13 | 58 | 11 |
| 3.0 M | 37[a] | 14 | 60[a] | 10 |

[a] Overlapping transitions.
[b] MB where stated, or else 0.01 M cacodylate pH 7.0. Salt concentrations are given as the molarity of the anion.

### 3.5. Thermodynamic analysis of triplex melting[3]

An aqueous solution of a triplex with no ionized base residues containing in addition one salt and one solute is described by the equilibria:

$$T \leftrightarrow D + SS_1 + \Delta n_{salt}salt + \Delta n_{solute}solute + \Delta n_{Water}water \quad (3 \rightarrow 2 + 1 \text{ transition}) \quad (1)$$

$$T \leftrightarrow SS_1 + SS_2 + SS_3 + \Delta n_{salt}salt + \Delta n_{solute}solute + \Delta n_{water}water$$
$$(3 \rightarrow 1 + 1 + 1 \quad \text{transition}) \quad (2)$$

where T, D, SS represent the triplex, duplex and single strand, respectively, and $\Delta n_{salt}$, $\Delta n_{solute}$, $\Delta n_{water}$ represent the release or uptake of salt, solute, and water on triplex dissociation. Since DNA is a polyanion, $\Delta n_{salt}$ implies $\Delta n_{cation}$. Using activities, their respective equilibrium constants are:

---

[3] Our analysis follows the approach of Wyman [6–8], which has been used variously to treat aspects of protein e.g. [9,10] and nucleic acid, e.g. [3,9,11] equilibria.
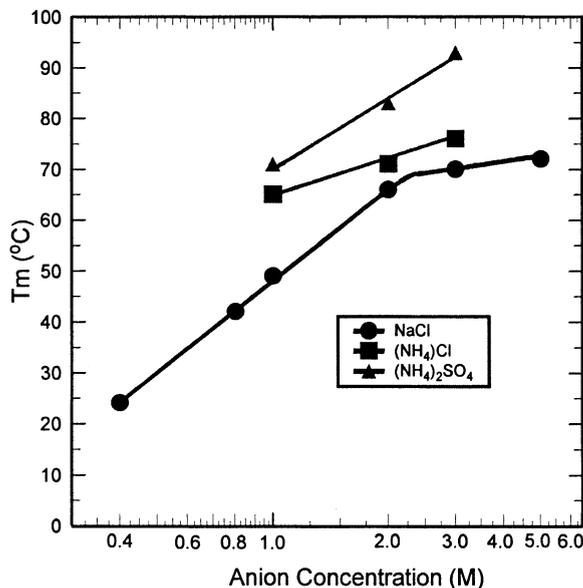
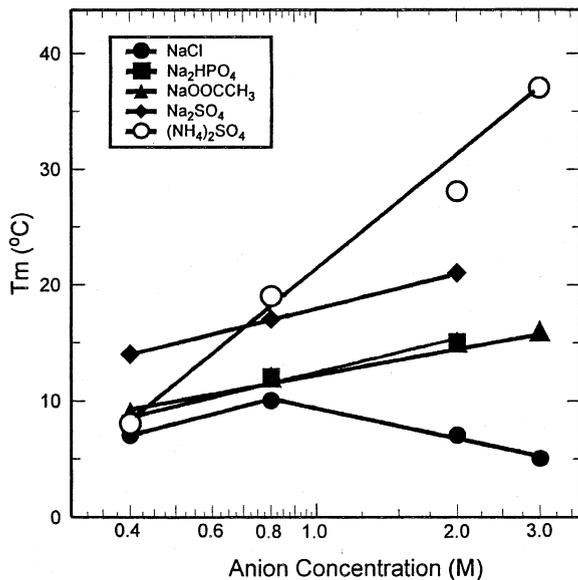Fig. 5. Dependence of $T_m$ on log anion concentration for $d(T)_{21} \cdot d(A)_{21} \cdot d(T)_{21}$ at pH 7.0.



Fig. 6. Dependence of $T_m$ on log anion concentration for $d(C^+\text{-}T)_6 \cdot d(A\text{-}G)_6 \cdot d(C\text{-}T)_6$ at pH 7.0.

$$K_1 = \frac{a_D \, a_{\text{SS1}} \, a_{\text{salt}}^{\Delta n \text{ salt}} \, a_{\text{solute}}^{\Delta n \text{ solute}} \, a_{\text{water}}^{\Delta n \text{ water}}}{a_T} \qquad (3)$$

$$K_2 = \frac{a_{\text{SS1}} \, a_{\text{SS2}} \, a_{\text{SS3}} \, a_{\text{salt}}^{\Delta n \text{ salt}} \, a_{\text{solute}}^{\Delta n \text{ solute}} \, a_{\text{water}}^{\Delta n \text{ water}}}{a_T} \qquad (4)$$

Converting to linear expressions gives:

$$\begin{aligned}
\ln K_1 = {} & \ln a_D + \ln a_{\text{SS1}} + \Delta n_{\text{salt}} \ln a_{\text{salt}} \\
& + \Delta n_{\text{solute}} \ln a_{\text{solute}} + \Delta n_{\text{water}} \ln a_{\text{water}} \\
& - \ln a_T
\end{aligned} \qquad (5)$$

$$\begin{aligned}
\ln K_2 = {} & \ln a_{\text{SS1}} + \ln a_{\text{SS2}} + \ln a_{\text{SS3}} \\
& + \Delta n_{\text{salt}} \ln a_{\text{salt}} + \Delta n_{\text{solute}} \ln a_{\text{solute}} \\
& + \Delta n_{\text{water}} \ln a_{\text{water}} - \ln a_T
\end{aligned} \qquad (6)$$

and leads to a series of expressions relating the change in the equilibrium constant on changing one parameter. For example, the expressions showing $K_1$ dependence on salt activity, or solute activity, or water activity are:

$$\begin{aligned}
\frac{\mathrm{d}(\ln K_1)}{\mathrm{d}(\ln a_{\text{salt}})} = {} & \frac{\mathrm{d}(\ln a_D)}{\mathrm{d}(\ln a_{\text{salt}})} + \frac{\mathrm{d}(\ln a_{\text{SS1}})}{\mathrm{d}(\ln a_{\text{salt}})} + \Delta n_{\text{salt}} \\
& + \frac{\Delta n_{\text{solute}} \; \mathrm{d}(\ln a_{\text{solute}})}{\mathrm{d}(\ln a_{\text{salt}})} \\
& + \frac{\Delta n_{\text{water}} \; \mathrm{d}(\ln a_{\text{water}})}{\mathrm{d}(\ln a_{\text{salt}})} \\
& - \frac{\mathrm{d}(\ln a_T)}{\mathrm{d}(\ln a_{\text{salt}})}
\end{aligned} \qquad (7)$$

$$\begin{aligned}
\frac{\mathrm{d}(\ln K_1)}{\mathrm{d}(\ln a_{\text{solute}})} = {} & \frac{\mathrm{d}(\ln a_D)}{\mathrm{d}(\ln a_{\text{solute}})} + \frac{\mathrm{d}(\ln a_{\text{SS1}})}{\mathrm{d}(\ln a_{\text{solute}})} \\
& + \frac{\Delta n_{\text{salt}} \; \mathrm{d}(\ln a_{\text{salt}})}{\mathrm{d}(\ln a_{\text{solute}})} + \Delta n_{\text{solute}} \\
& + \frac{\Delta n_{\text{water}} \; \mathrm{d}(\ln a_{\text{water}})}{\mathrm{d}(\ln a_{\text{solute}})} \\
& - \frac{\mathrm{d}(\ln a_T)}{\mathrm{d}(\ln a_{\text{solute}})}
\end{aligned} \qquad (8)$$

$$\frac{d(\ln K_1)}{d(\ln a_{\text{water}})} = \frac{d(\ln a_{\text{D}})}{d(\ln a_{\text{water}})} + \frac{d(\ln a_{\text{SS1}})}{d(\ln a_{\text{water}})}$$
$$+ \frac{\Delta n_{\text{salt}}\ d(\ln a_{\text{salt}})}{d(\ln a_{\text{water}})}$$
$$+ \frac{\Delta n_{\text{solute}}\ d(\ln a_{\text{solute}})}{d(\ln a_{\text{water}})}$$
$$+ \Delta n_{\text{water}} - \frac{d(\ln a_T)}{d(\ln a_{\text{water}})} \qquad (9)$$

Since $\ln K = \dfrac{-\Delta H^{\text{o}}}{RT} + \dfrac{\Delta S^{\text{o}}}{R}$ and

$$d(\ln K) = \frac{-\Delta H^{\text{o}}}{R}\, d(T^{-1}) \qquad (10)$$

we obtain a series of expressions relating triplex thermal stability to changes in salt activity, solute activity, and water activity, thus:

$$\frac{d(\ln K_1)}{d(\ln a_{\text{salt}})} = \frac{-\Delta H^{\text{o}}}{R}\, \frac{d(T_{m^{-1}})}{d(\ln a_{\text{salt}})}$$
$$= \frac{d(\ln a_{\text{D}})}{d(\ln a_{\text{salt}})} + \frac{d(\ln a_{\text{SS1}})}{d(\ln a_{\text{salt}})} + \Delta n_{\text{salt}}$$
$$+ \frac{\Delta n_{\text{solute}}\ d(\ln a_{\text{solute}})}{d(\ln a_{\text{salt}})}$$
$$+ \frac{\Delta n_{\text{water}}\ d(\ln a_{\text{water}})}{d(\ln a_{\text{salt}})}$$
$$- \frac{d(\ln a_T)}{d(\ln a_{\text{salt}})} \qquad (11)$$

$$\frac{d(\ln K_1)}{d(\ln a_{\text{solute}})} = \frac{-\Delta H^{\text{o}}}{R}\, \frac{d(T_{m^{-1}})}{d(\ln a_{\text{solute}})}$$
$$= \frac{d(\ln a_{D})}{d(\ln a_{\text{solute}})} + \frac{d(\ln a_{\text{SS1}})}{d(\ln a_{\text{solute}})}$$
$$+ \frac{\Delta n_{\text{salt}}\ d(\ln a_{\text{salt}})}{d(\ln a_{\text{solute}})} + \Delta n_{\text{solute}}$$
$$+ \frac{\Delta n_{\text{water}}\ d(\ln a_{\text{water}})}{d(\ln a_{\text{solute}})}$$
$$- \frac{d(\ln a_T)}{d(\ln a_{\text{solute}})} \qquad (12)$$

$$\frac{d(\ln K_1)}{d(\ln a_{\text{water}})} = \frac{-\Delta H^{\text{o}}}{R}\, \frac{d(T_{m^{-1}})}{d(\ln a_{\text{water}})}$$
$$= \frac{d(\ln a_{\text{D}})}{d(\ln a_{\text{water}})} + \frac{d(\ln a_{\text{SS1}})}{d(\ln a_{\text{water}})}$$
$$+ \frac{\Delta n_{\text{salt}}\ d(\ln a_{\text{salt}})}{d(\ln a_{\text{water}})}$$
$$+ \frac{\Delta n_{\text{solute}}\ d(\ln a_{\text{solute}})}{d(\ln a_{\text{water}})}$$
$$+ \Delta n_{\text{water}} - \frac{d(\ln a_T)}{d(\ln a_{\text{water}})} \qquad (13)$$

Eqs. (11)–(13) are more commonly used in the form

$$\frac{-\Delta H^{\text{o}}}{R}\, \frac{d(T_{m^{-1}})}{d(\ln\ [\text{salt}])} = \Delta n_{\text{salt}} \qquad (14)$$

$$\frac{-\Delta H^{\text{o}}}{R}\, \frac{d(T_{m^{-1}})}{d(\ln[\text{solute}])} = \Delta n_{\text{solute}} \qquad (15)$$

$$\frac{-\Delta H^{\text{o}}}{R}\, \frac{d(T_{m^{-1}})}{d(\ln a_{\text{water}})} = \Delta n_{\text{water}} \qquad (16)$$

where all the other terms are considered equal to zero, and concentration is used in place of activity for salts and solutes.[4]

### 3.6. Salt Dependence for $d(T)_{21}$: $d(A)_{21}\cdot d(T)_{21}$

We now evaluate $\Delta n_{\text{salt}}$ and consider the use of Eq. (11) and Eq. (14). In order to determine $\Delta n_{\text{salt}}$, the enthalpy change associated with triplex melting

---

[4] In Eq. (15), $\Delta n_{\text{solute}}$ represents the uptake or release of solute associated with a macromolecular transition. We consider here two classes of solution additives that stabilize nucleic acid triplexes. One class includes positively charged ions that act as counterions or 'salts' to the polyanionic nucleic acid strands of a triplex. The other class includes solutes that do not interact with nucleic acid acid strands. Such solutes most likely exert their effect on triplex structure by affecting $a_{\text{water}}$, so that one is indirectly measuring $\Delta n_{\text{water}}$ and not $\Delta n_{\text{solute}}$. Of course, at the high concentration at which the tetramethyammonium cation is used, it probably exerts its effect both as a counterion and as a solute affecting $a_{\text{water}}$. In any case, until there is evidence e.g. [12] to show that a solute does or does not interact with the triplex (or other macromolecule), it would be prudent not to calculate $\Delta n_{\text{solute}}$ or $\Delta n_{\text{water}}$. For example, do methanol, ethanol and propanol interact directly with duplexes and triplexes ($\Delta n_{\text{solute}}$) or do they only change $a_{\text{water}}$, i.e. $\Delta n_{\text{water}}$?

is needed. Fig. 4 shows that this triplex undergoes a $3 \rightarrow 2+1$ dissociation in 0.8 M NaCl. If $C_t$ is the total concentration of duplex + single strand available to form triplex, and $\alpha$ is the fraction that forms triplex, then the observed equilibrium constant is

$$K = \frac{(1-\alpha)^2 \frac{C_t}{2}}{\alpha}$$

where

$$\alpha = \frac{A(\text{duplex}+\text{coil})_{260} - A_{260}}{A(\text{duplex}+\text{coil})_{260} - A(\text{triplex})_{260}} \qquad (17)$$

and $K$ is obtained from the equilibrium between the triplex and core duplex + third strand. The hyperchromic change at 260 nm is a measure of the dissociation of triplex: $A(\text{triplex})_{260}$ is the absorbance of intact triplex; $A(\text{duplex}+\text{coil})_{260}$ is the sum of the absorbances of duplex and single strand; $A_{260}$ is the absorbance at any temperature within the transition.

From Eq. (10) and a plot of $\ln K$ vs. $1/T$, a van't Hoff enthalpy of 3.3 kcal mol$^{-1}$ Hoogsteen T:A base pair (Fig. 7) is obtained, in good agreement with the calorimetrically determined value of 3.4 kcal mol$^{-1}$ Hoogsteen T:A base pair [11]. In 2.0 M NaCl, Fig. 4 shows that this triplex undergoes $3 \rightarrow 1+1+1$ dissociation. If $C_t$ is the total concentration of single strands available to form triplex, then the observed equilibrium constant is

$$K = \frac{(1-\alpha)^3 \frac{C_t^2}{9}}{\alpha}$$

where

$$\alpha = \frac{A(\text{coil})_{260} - A_{260}}{A(\text{coil})_{260} - A(\text{triplex})_{260}} \qquad (18)$$

and $K$ is obtained from the equilibrium between the triplex and single strands, and $A(\text{coil})_{260}$ is the absorbance of the single strands.

Since this is a $3 \rightarrow 1+1+1$ transition, the enthalpy change is the sum of the enthalpy changes for the
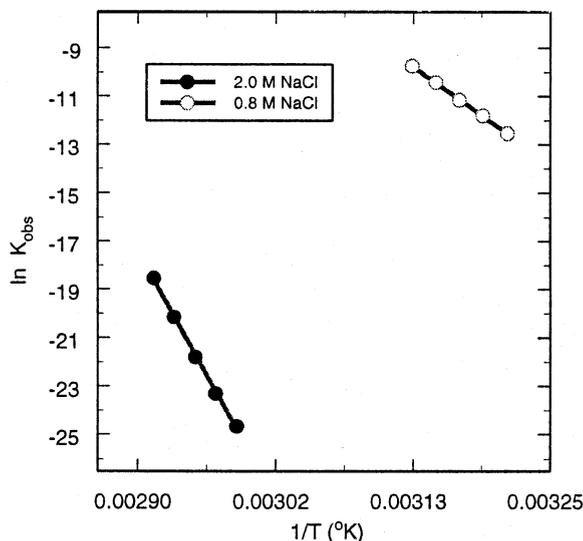


Fig. 7. ln K vs. $1/T$ for dissociation of the triplex $d(T)_{21}$:$d(A)_{21}$•$d(T)_{21}$ in 0.8 M and 2.0 M NaCl at pH 7.0. In 0.8 M NaCl, the slope of $-34653.5$ K yields $\Delta H° = 68925$ cal mol$^{-1}$ third strand or 3.3 kcal mol$^{-1}$ Hoogsteen T:A base pairs. In 2.0 M NaCl, the steeper slope of $-87806.6$ K yields $\Delta H° = 174640$ cal mol$^{-1}$ triplex or 8.32 kcal mol$^{-1}$ triplet T:A•T base pairs.

Hoogsteen base pairs formed by the third strand and the Watson–Crick duplex base pairs. From the straight line fit in Fig. 7, this enthalpy change is 8.32 kcal mol$^{-1}$ T:A•T base triplet. If the calorimetrically determined enthalpies [11] for the two separate transitions are added, i.e. that for the dissociation of the Hoogsteen T:A base pair (3.4 kcal mol$^{-1}$) and that for dissociation of the Watson-Crick A•T base pair (6.9 kcal mol$^{-1}$)], then the van't Hoff enthalpy of 8.32 kcal mol$^{-1}$ T:A•T base triplet is less than the sum of the individual steps by 2 kcal. This difference implies that the heat capacities of the triplex, duplex + single strand, and the three single strands are unequal.

For Eq. (11), the slope of a plot of $T_m^{-1}$ vs. $\ln a_{\text{salt}}$ is needed, where $T_m$ is the triplex dissociation temperature and $a_{\text{salt}}$ is the salt activity in the solution at that temperature. Since the triplex concentration is $\sim 4 \times 10^{-5}$ M (nucleic acid residue $\sim 2 \times 10^{-3}$ M), in NaCl solutions ranging from 0.4 to 5.0 M, we have used the known NaCl activity coefficients in water [13] to approximate the NaCl activity in the
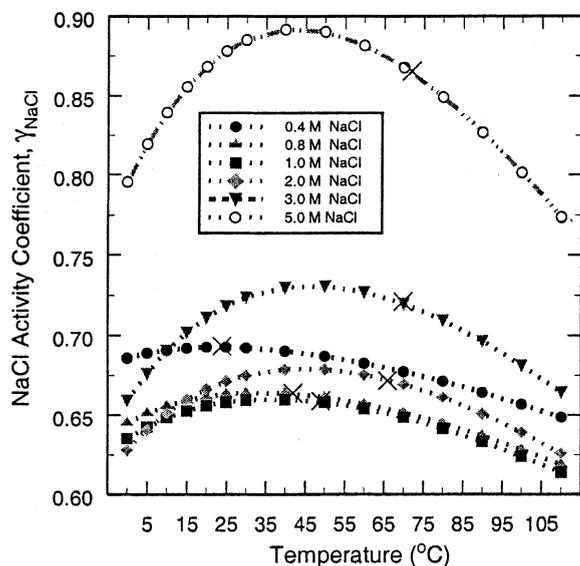
Fig. 8. Temperature-dependence of NaCl activity coefficient, $\gamma_{NaCl}$, at different NaCl concentrations [13]. Third strand or triplex melting temperatures are indicated by X.

triplex solutions. Fig. 8 shows the temperature dependence of the NaCl activity coefficient and the values that were used to determine $a_{NaCl}$. The data in Fig. 8 show large deviations from $\gamma = 1$ and highlight the limitation in using Eq. (14), which assumes $\gamma = 1$. For example, a 0.4 M NaCl solution at 25 °C has a significantly reduced activity of 0.277. In addition, the practice of plotting $T_m^{-1}$ vs. ln [salt] and then multiplying the slope by some *constant* to take non-ideality into account for *all* the terms in Eq. (11) should be done with caution, as the activity coefficients for salts (e.g. Fig. 8), solutes and water are not linear with respect to temperature.

The $a_{NaCl}$ values were then used to plot $T_m^{-1}$ vs. ln $a_{NaCl}$. Fig. 9a shows that straight line fits were obtained by separating the data into two groups: 0.4–1.0 M and 2.0–5.0 M NaCl, which correspond to the $3 \rightarrow 2 + 1$ and $3 \rightarrow 1 + 1 + 1$ triplex transitions, respectively (Fig. 4). These results are consistent in that the salt concentration ranges over which two different pathways were spectroscopically identified for triplex dissociation also display two thermodynamically different salt dependences.
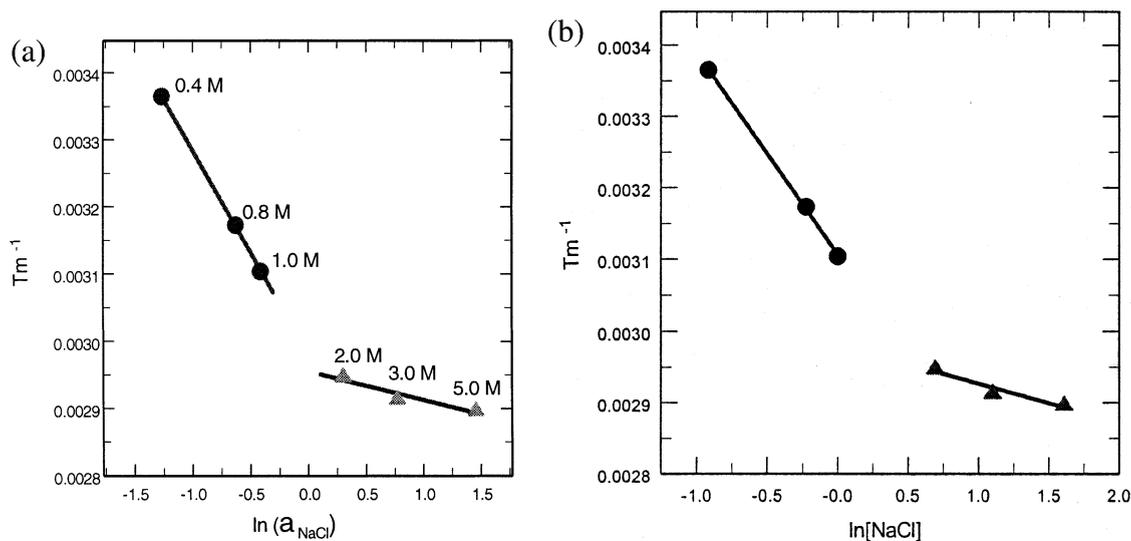


Fig. 9. (a) $T_m^{-1}$ is the inverse third strand or triplex dissociation temperature and $a_{NaCl}$ is the NaCl activity in water at the dissociation temperature (as obtained from Fig. 8). Linear regressions give a slope of $-3.0 \times 10^{-4}$ K$^{-1}$ for low salt and $-4.3 \times 10^{-5}$ K$^{-1}$ for high salt. (b) $T_m^{-1}$ vs. ln[NaCl]. Linear regressions give a slope of $-2.8 \times 10^{-4}$ K$^{-1}$ for low salt and $-5.5 \times 10^{-5}$ K$^{-1}$ for high salt.
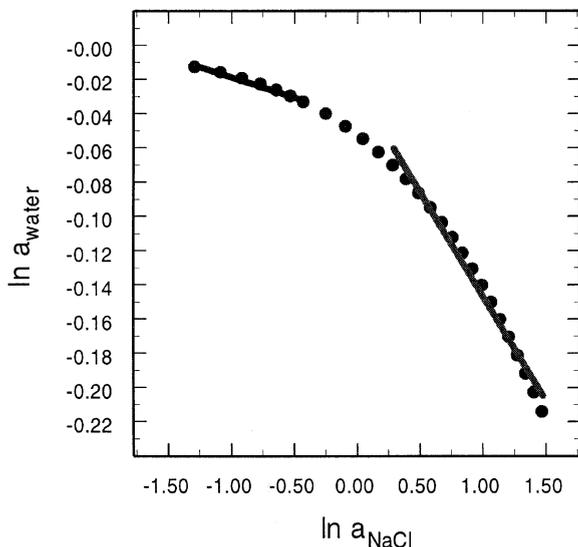
Fig. 10. $\ln a_{\text{water}}$ vs. $\ln a_{\text{NaCl}}$ at 25 °C. Linear regression between 0.4 and 1.0 M NaCl gives a slope of $-2.3 \times 10^{-2}$ and between 2.0 and 5.0 M NaCl gives a slope of $-1.2 \times 10^{-1}$.

The next term we address in Eq. (11) is $\dfrac{d(\ln a_{\text{water}})}{d(\ln a_{\text{salt}})}$. It is expected that this term will be small since the NaCl concentration changes significantly. Fig. 10 shows that between 0.4 and 5.0 M NaCl this term is non-linear; however, a linear fit is obtained by separating the data into two groups: $\sim 0.4–1.0$ M and $\sim 2.0–5.0$ M NaCl. Since the slope of the high salt domain is five times that of the low salt domain, this implies that the (relatively) larger change in water activity may play a role in changing the triplex transition pathway from $3 \rightarrow 2+1$ to $3 \rightarrow 1+1+1$.

The changes in activity of single strand, duplex and triplex as a function of salt activity have not been determined, and in this analysis they are assumed to be small. Moreover, there are no solute additives present, so $\dfrac{d(\ln a_{\text{solute}})}{d(\ln a_{\text{Nacl}})} = 0$, and Eq. (11) simplifies to:

$$\frac{-\Delta H^{\circ}}{R} \frac{d(T_{m^{-1}})}{d(\ln a_{\text{NaCl}})} = \Delta n_{\text{NaCl}}$$

$$+ \Delta n_{\text{water}} \frac{d(\ln a_{\text{water}})}{d(\ln a_{\text{NaCl}})} \quad (19)$$

($\Delta n_{\text{salt}}$ or $\Delta n_{\text{NaCl}}$ for DNA and RNA implies $\Delta n_{\text{Na}^+}$).

In the low salt domain, $0.4-1.0$ M NaCl, where the triplex transition is $3 \rightarrow 2+1$, Eq. (19) gives $0.50 = \Delta n_{\text{Na}^+} + \Delta n_{\text{water}} (-2.3 \times 10^{-2})$. Since $\Delta n_{\text{water}}$ values are between 0.5 and 2 per dT residue, the second term, $\Delta n_{\text{water}}$, is small; omitting it, we obtain $\Delta n_{\text{Na}^+} = 0.5$ (or using the lower and upper $\Delta n_{\text{water}}$ values of 0.5 and 2, $\Delta n_{\text{Na}^+} = 0.49$ and 0.45. Notice that taking into account the change in $a_{\text{water}}$ with increasing salt concentration results in a lower $\Delta n_{\text{Na}^+}$). Hence, the counterion rearrangement for the transition $d(T)_{21} \colon d(A)_{21} \bullet d(T)_{21} \rightarrow d(T)_{21} + d(A)_{21} \bullet d(T)_{21}$ results in a release of 0.5 $Na^+$ to bulk solution per dT residue or 10.5 $Na^+$ per third strand. This value of 0.5 $Na^+$ released is in good agreement with that of Spink and Chaires [11] obtained using their Eq. (7) and values from their Table 2:

$$\frac{-\Delta H^{\circ}}{R} \frac{d(T_{m^{-1}})}{d(\ln [\text{salt}])} = \alpha \Delta n_{\text{Na}^+}$$

$$\frac{-3360}{R} (-2.92 \times 10^{-4}) = 0.9 \, \Delta n_{\text{Na}^+}$$

giving $\Delta n_{\text{Na}^+} = 0.55$ for poly(dT)$\colon$poly(dA)$\bullet$poly(dT) between 0.14 and 0.29 M NaCl.

Our observed value can also be compared with calculated $\Delta n_{\text{Na}^+}$ values based on Manning's counterion condensation theory [3,14–16], where the fraction of counterion condensation per charge is obtained using

$$\theta = 1 - \frac{1}{\xi} \quad (20)$$

where

$$\xi = \frac{e^2}{b \varepsilon \, kT} \quad (21)$$

and $b$ is the average inter-phosphate spacing, $e$ is the charge of the electron, $\varepsilon$ is the solvent dielectric constant, $k$ is the Boltzmann constant and $T$ is the absolute temperature.

Since the dielectric constant is temperature- and salt type- and concentration-dependent, we have used [17,18]

$$\varepsilon = \varepsilon_w + 2\delta C \quad (22)$$

Table 3
Counterion condensation for $d(T)_{21}$:$d(A)_{21}$•$d(T)_{21}$

| [NaCl] | $T_m$ (°K) | $\varepsilon_w$ | $\varepsilon^a$ | $\xi_T$ | $\xi_D$ | $\xi_{SS}$ | $\Delta\Theta_{(per\ mole\ triplex)}$ | $Na^+_{(released)}$ |
|---|---|---|---|---|---|---|---|---|
| 0.4 M | 297.15 | 79 | 75 | 6.61 | 4.41 | 2.20 | −9.1 | 9.1 |
| 0.8 M | 315.15 | 72 | 63 | 7.42 | 4.95 | 2.47 | −8.1 | 8.1 |
| 1.0 M | 322.15 | 70 | 59 | 7.75 | 5.17 | 2.58 | −7.7 | 7.7 |

[a] Calculated using Eq. (22).

to obtain more accurate $\varepsilon$ values, where $\delta$ is the molar depression caused by a salt ($\delta = -5.5$ for NaCl at 25 °C) and $C$ is the molar concentration of salt. Since Eq. (22) has been shown to be valid for salt concentrations below 2 M, Table 3 lists the temperature dependent $\varepsilon_w$ and salt dependent $\varepsilon$ values in 0.4, 0.8, and 1.0 M NaCl. Table 3 also gives values for $\Delta\Theta_{(per\ mole\ triplex)}$, the change in counterion condensation for the melting of $d(T)_{21}$:$d(A)_{21}$•$d(T)_{21}$ by a $3 \rightarrow 2+1$ transition calculated using:

$$\Delta\Theta_{(3 \rightarrow 2+1)} = \Theta_D + \Theta_{ss} - \Theta_T$$
$$= \left[\left(1 - \frac{1}{\xi D}\right)40\right] + \left[\left(1 - \frac{1}{\xi SS}\right)20\right]$$
$$- \left[\left(1 - \frac{1}{\xi T}\right)60\right] \qquad (23)$$

where each strand has 20 phosphates and $b_{(single\ strand)} = 3.4$ Å, $b_{(duplex)} = \dfrac{3.4\ \text{Å}}{2}$ and $b_{(triplex)} = \dfrac{3.4\ \text{Å}}{3}$.

The calculated value for $\Delta\Theta$ of $-9.1$ $Na^+$ for the change in counterion condensation on triplex melting in 0.4 M NaCl agrees very well with our observation of 10.5 $Na^+$ released per third strand. The $\Delta\Theta$ values of $-8.1$ (0.8 M NaCl), and $-7.7$ (1.0 M NaCl) also confirm the trend of decreasing $Na^+$ release at higher salt concentrations. As far as we are aware, this is the first time that the temperature and salt dependent dielectric constant has been used to show the effect on counterion condensation, and decreasing $\Delta n_{Na^+}$ with increasing NaCl concentration.

Knowing $\Delta H°$ and the melting temperature (in 0.8 M NaCl $T_m = 42$ °C), the total entropy change per third strand residue can be calculated from $\Delta S° = \dfrac{\Delta H°}{T_m} \approx 10$ cal.K$^{-1}$.mol$^{-1}$ dT residue. The $Na^+$ contribution can also be estimated knowing that it acts as a screening counterion that is not site bound, but does have restricted motion on the surface of a cylindrical shell (two-dimensional) relative to bulk $Na^+$, which has three-dimensional freedom. In this simple model we assume the hydration of the $Na^+$ to be essentially unchanged, while its translational degrees of freedom increase from 2 to 3. Using this and the result of 0.5 $Na^+$ released per dT residue, we obtain $\Delta S°_{Na^+} = 0.5$ ($R$ ln 3/2) = 0.4 cal K$^{-1}$ mol$^{-1}$ dT residue or 4% of the total entropy change. Re-expressing this in terms of the $Na^+$ entropic contribution to the free energy change, we obtain— $T_m \Delta S°_{Na^+} \cong -130$ cal mol$^{-1}$ dT residue. Even if one considers DNA-$Na^+$ counter-ions as having restricted motion along one dimension, then $\Delta S°_{Na^+} = 0.5$ ($R$ ln 3/1) = 1.1 cal K$^{-1}$ mol$^{-1}$ dT residue, with the $Na^+$ contribution to the total entropy change ranging from 4 to 11%.

In the high salt domain, 2.0–5.0 M NaCl, in which the triplex dissociates $3 \rightarrow 1+1+1$, Eq. (19) gives $0.18 = \Delta n_{Na^+} + \Delta n_{water}$ ($-1.2 \times 10^{-1}$), and the second term cannot be ignored. Using the lower and upper $\Delta n_{water}$ values of 0.5 and 2, $\Delta n_{Na^+} = 0.24$ and 0.42, respectively, or 5.0 and 8.8 $Na^+$ per third strand. Although a more accurate $\Delta n_{Na^+}$ value cannot be determined due to the larger $\dfrac{d(\ln a_{water})}{d(\ln a_{NaCl})}$ term, a lower $\Delta n_{NaCl}$ value is expected, because at these high NaCl concentrations, triplex stability is less sensitive to changes in NaCl concentration.

We can also compare the results obtained using Eq. (11) with those obtained with the more com-

monly employed Eq. (14), for which the slopes of the plots of $T_m^{-1}$ vs. ln[NaCl] (Fig. 9b) yield $\Delta n_{Na^+} = 0.46$ in the lower salt range and 0.23 in the higher salt range. The low salt value is in good agreement with the $\Delta n_{Na^+}$ value of 0.5, for which the concentration and temperature dependences of the activity of NaCl were taken into account as well as the dependence of water activity on NaCl activity. Until experiments, e.g. [19,20] are performed to determine the change in the activities of single strand, duplex and triplex as a function of salt activity, it is difficult to estimate their contribution. However, for this triplex and NaCl in the 0.4–1.0 M range, the simplified Eq. (14) does work, which could be, because the salt activity terms cancel or that Eq. (14) is valid up to 1.0 M NaCl. We favor the latter explanation, because the triplex undergoes a $3 \rightarrow 2+1$ transition up to 1.0 M NaCl and a $3 \rightarrow 1+1+1$ transition between 2.0 and 5.0 M NaCl; Fig. 10 shows a weaker effect on $a_{water}$ between 0.4 and 1.0 M NaCl and a significantly stronger effect between 2.0 and 5.0 M NaCl; and the triplex melting temperatures measured in 0.4, 0.8 and 1.0 M NaCl (Fig. 8) actually correspond to the narrow range of 0.65–0.70 of $\gamma_{NaCl}$.

### 3.7. Changes in $\Delta n_{water}$ during transitions for $d(T)_{21} \cdot d(A)_{21} \cdot d(T)_{21}$

Since $\dfrac{d(T_{m^{-1}})}{d(\ln a_{water})}$ and other terms in Eq. (13) are unknown, $\Delta n_{water}$ cannot be explicitly calculated. However, we can qualitatively evaluate whether it is positive or negative upon dissociation of the triplex. One might have thought that on triplex melting, removal of a third strand from the major groove would result in a net uptake of water. However, the following result clearly indicates a net release of water on third strand dissociation. In 2.0 M NaCl the $T_m$ value is 66 °C, while in 2.0 M NaClO₄ it is 44 °C. This difference is explained by a net release of water to the more disordered bulk water in the presence of ClO₄⁻, resulting in a larger $\Delta S^{\circ}_{water}$, and if $\Delta H^{\circ}$ for dissociation of the third strand is independent of salt type, a lower $T_m$. By definition, the mid-point of the triplex dissociation, i.e. $T_m$, occurs when $\Delta G^{\circ} = \Delta H^{\circ} - T_m \ \Delta S^{\circ} = 0$, resulting in $\Delta H^{\circ} =$

$T_m \ \Delta S^{\circ}$. In that case, a larger positive $\Delta S^{\circ}$ value must result in a lower $T_m$ value. The net release of water on triplex melting could result from the higher triplex charge density being associated with more water of hydration.

Using the data for the 2.0 M Na⁺ salts, we can also compare the relative differences in $\Delta S^{\circ}$ for the anions:

$$\Delta S^{\circ} = \frac{\Delta H^{\circ}}{T_m} = \frac{8316 \ \text{cal mol}^{-1} \ \text{triplet T} \colon \text{A} \cdot \text{T}}{T_m(\text{K})}$$

$= 23.5 \ (SO_4^{2-})$, $24.5 \ (Cl^-)$, $26.2 \ (ClO_4^-)$. These values show that relative to Cl⁻, the water structure-making $SO_4^{2-}$ lowers $\Delta S^{\circ}$ by $-1.0$ cal $K^{-1}.mol^{-1}$ T$\colon$A$\cdot$T base triplets, while the water structure breaking $ClO_4^-$ raises $\Delta S^{\circ}$ by 1.7 cal $K^{-1}.mol^{-1}$ T$\colon$A$\cdot$T base triplets.[5] What do these observed $\Delta\Delta S^{\circ}$ values represent? If we make the assumption that the change in entropy for the triplex dissociating to single strands is the same for all these 2.0 M salts as is the change in entropy due to released Na⁺, then the only remaining difference must be the entropy associated with water release on triplex melting in the presence of an entropy raising or lowering water anion. That is, for $ClO_4^-$, the positive $\Delta\Delta S^{\circ}$ value of 1.7 cal $K^{-1}.mol^{-1}$ T$\colon$A$\cdot$T base triplets represents the increase in entropy for the water released per T$\colon$A$\cdot$T base triplets in the presence of 2.0 M $ClO_4^-$ vs. 2.0 M Cl⁻. For $SO_4^{2-}$ the negative $\Delta\Delta S^{\circ}$ value of $-1.0$ cal $K^{-1}.mol^{-1}$ T$\colon$A$\cdot$T base triplets represents the decrease in entropy for the water released per T$\colon$A$\cdot$T base triplets in the presence of 2.0 M $SO_4^{2-}$ vs. 2.0 M Cl⁻. These results provide quantitative support for the qualitative statement of the Hofmeister series that at high salt concentrations triplex stability follows the water structure-making anions.

## 4. Discussion

### 4.1. The Hofmeister effect

When a salt is dissolved in water, different anions and cations decrease, increase or have little effect on the volume of the solution [22a,23].

---

[5] These high 2 M salt concentrations preclude the application of the insightful analysis of Rau and Parsegian [21], in which they calculated the entropic differences between Mn(ClO₄)₂ and MnCl₂ bulk solutions at 50 mM salt for the release of 1 mol of water.

These alternative effects have been rationalized in terms of the interaction of the anion or cation with immediately surrounding water molecules according to what is often called the multilayer hydration model [22b].[6] Briefly, this model of ion–water interaction divides the volume of an ion in solution, $V_{ion}$, into four components:

$$V_{ion} = V_{cryst} + V_{elect} + V_{disord} + V_{caged}$$

where $V_{cryst}$ is the volume of the ion based on its crystal radius; $V_{elect}$ is the electrostriction volume (stronger ion-$H_2O$ interaction decreases the volume); $V_{disord}$ is the disordered or void-space volume (weaker ion–$H_2O$ interaction increases the volume); and $V_{caged}$ is the caged or structured volume that occurs when a hydrophobic ion (organic cation) interacts with $H_2O$ molecules, decreasing the volume.

Although these ion volume factors are interdependent, they afford a useful empirical classification of ions based upon the changes in solution volume when the ions are added to water. Ions are described as electrostrictive 'structure-making' when $V_{elect}$ is dominant, as disordered 'structure-breaking' when $V_{disord}$ is dominant, and as hydrophobic 'structure-making' when $V_{caged}$ is dominant.

The structure-making or structure-breaking tendency of anions based upon this model follows the rank order of the Hofmeister series, which is the relative tendency of anions to stabilize and solubilize proteins. These effects [23] were first noted in a classic paper by Hofmeister [25], in which he ranked the effect of anions on protein solubility, including:

(destabilize proteins) $ClO_4^- < Cl^- < CH_3COO^-$
$< HPO_4^{2-} < SO_4^{2-}$ (stabilize proteins)
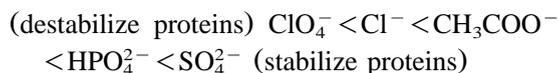
This rank order was subsequently called the 'chaotropic series', as extensive studies showed $Cl^-$ to have little effect on water-structure, whereas anions to the left of it are water structure-breakers ($V_{disord}$ is dominant) or *chaotropes* (from the Greek *chao*, meaning disorder), because they destabilize proteins, while anions to the right of $Cl^-$ are water structure-makers ($V_{elect}$ is dominant) or *kosmotropes* (from the Greek *kosmos*, meaning order), because they stabilize proteins. Many experimental observations [23] indicate that polar or charged chaotropes 'disrupt' the folded state of proteins, because they interact with water less strongly, but with the peptide bond more strongly, inducing the unfolded state. In contrast, polar or charged kosmotropes stabilize the folded state of proteins, because they interact with water more strongly than bulk water molecules with each other.

In this study, where the anions are unlikely to interact with the highly negatively charged triplexes, it is (as discussed in Section 3.7) the triplex water of hydration that contributes to triplex stability in the presence of water structure-making anions or detracts from triplex stability in the presence of water structure-breaking anions. The direct measurement of rotational motion of water molecules in the hydration spheres of various anions by Endom et al. [24] gives clear meaning to the terms water structure-making and -breaking anions.[7]

---

[6] Since it is difficult to discuss the components $V_{cryst}$, $V_{elect}$, $V_{disord}$ and $V_{caged}$ that make up $V_{ion}$ as true separate parameters, particularly so for $V_{elect}$, $V_{disord}$ and $V_{caged}$, which are very difficult to measure as separate experimental observables, it is the partial molal volume, which equals $V_{ion} - V_{cryst}$, that is most often discussed. In other words, a negative partial molal volume means that the volume occupied by an ion in solution is smaller than its volume in a crystal lattice; such an ion is referred to as structure-making. This reduced volume is attributed to the three (interdependent) terms $V_{elect}$, $V_{disord}$ and $V_{caged}$. That is, partial molal volume $= V_{ion} - V_{cryst} = V_{elect} + V_{disord} + V_{caged}$. From p. 544 of [22], 'Positive B coefficients, negative partial molal volumes, and negative partial molal entropies are normally associated with the electrostrictive structure-making ions, whereas negative B coefficients, positive partial molal volumes and positive partial molal entropies are normally associated with structure-breaking ions.'

[7] Endom et al. [24] have measured the mobility of water in salt solutions by NMR and determined the activation energies (kcal/mol) between 35–80 °C for the rotational motion of water molecules in the hydration spheres of $F^-$ (4.3), $Cl^-$ (3.3), $Br^-$ (2.9) and $I^-$ (2.7) relative to that of pure water (3.3). Note that the activation energy for the rotational motion of water molecules in the hydration sphere of $Cl^-$ is the same as that of pure water, so that $Cl^-$ is considered neither a water structure-breaker (chaotrope) nor a water structure-maker (kosmotrope). Also, the trend for these halides of increasing rotational motion for water of hydration follows our calculated values of their decreasing effective surface charge density. Unfortunately, Endom et al. did not study the rotational motion for water of hydration around $ClO_4^-$, $HPO_4^{2-}$ and $SO_4^{2-}$.

### 4.2. A surface phenomenon model for the Hofmeister effect

To quantitatively evaluate this mechanistic model, we have treated the anion–$H_2O$ interaction as a surface phenomenon, and calculated the effective surface charge density for each anion. Table 4 shows that the rank order based upon their effective surface charge densities follows that of the Hofmeister series:

$$ClO_4^- < I^- < Br^- < Cl^- < HPO_4^{2-} < SO_4^{2-}$$

It is customary to rank the Hofmeister series in terms of anion concentration even though these anions differ in valency, so that their salts contribute differently to total ionic strength. However, ranking the Hofmeister series in terms of ionic strength is inappropriate, because ionic strength depends on *free ion* rather than total salt concentration; and free ion concentration decreases with increasing salt concentration, i.e. activity coefficient < 1. Consequently, it might be more appropriate to rank order monovalent and divalent anions separately, especially since the strength of the anion–$H_2O$ interaction is clearly charge dependent. In fact, our calculations indicate that the surface charge density of an anion correlates well with its effect on the thermal stability of proteins, and nucleic acid duplexes and triplexes (Table 4). This correlation is meaningful in that a stronger effective surface charge density gives rise to a stronger ion-water interaction that results in more ordered water.[8] Thus, there is a direct link

between an atomic model (stronger ion–water interaction) and a macroscopic (thermodynamic) model (decrease water entropy). For example, $ClO_4^-$ with lower effective surface charge density should permit increased rotational and translational motion of the surrounding water.[9]

The correlation then, of surface charge density with thermal stability of proteins and nucleic acids, implies that for the inorganic anions, $V_{elect}$ and $V_{disord}$ must be the dominant factors that give rise to the Hofmeister effect.

### 4.3. A Hofmeister anion effect on DNA stability

Hamaguchi and Geiduschek [26] have shown that the effect of various salts on the stability of natural DNAs follows the Hofmeister series, with the minor exception of $CH_3COO^-$, which they ranked one before instead of one after $Cl^-$. They observed, for example, that sea urchin DNA in 4.0 M sodium salt at pH 7.0 has a $T_m$ value (°C) of 74° in $ClO_4^-$, < 84° in $CH_3COO^-$, < 90° in $Cl^-$. They also found that at the very high salt concentrations needed to observe the anion effects, there are only minor differences in the $T_m$ value when the cations are $Li^+$, $Na^+$ or $K^+$.

Parenthetically, we note that consistent with the results of other studies showing preferential stabilization of nucleic acid interactions by $NH_4^+$ over $Na^+$ [27], we observe slightly higher triplex stabilities, e.g. for $d(T)_{21} \cdot d(A)_{21} \cdot d(T)_{21}$ in 2.0 M $NH_4Cl$ vs. NaCl ($T_m$ 71 °C vs. 66 °C) and in $(NH_4)_2 SO_4$ vs. $Na_2SO_4$ ($T_m$ 83 °C vs. 80 °C).

### 4.4. Anion stabilization of triplexes follows the Hofmeister series

Table 5 shows that the rank order for stabilization of the two triplexes we studied is the same in 2.0 M anion at pH 7, i.e. $ClO_4^- < Cl^- < CH_3COO^- < HPO_4^{2-} < SO_4^{2-}$. However, anion stabilization, i.e. $dT_m/d \log[\text{anion}]$ is much greater for the triplex with no charged residues in the third strand. This is not unexpected given the negative effect of total ionic strength observed for NaCl on

---

[8] The interpretation of the calculated effective surface charge density value is then one of anion–water interaction, where the more negative the charge density of the anion, the stronger the anion–water interaction. This scale could be converted to negative values (chaotropes) and positive values (kosmotropes) by subtracting the value for each anion from the value for chloride. This adjusted scale would be analogous to Jones–Dole viscosity B coefficients, which are the result of an adjustable (fitting) parameter in the Jones–Dole viscosity equation that has been interpreted to imply strong hydration when B is positive (kosmotrope) and weak hydration when B is negative (chaotrope). However, the semiempirical Jones–Dole equation is only valid for salt concentrations up to approximately 0.1 M. The known viscosity B values do not predict the exact rank order, and there are no published values for the phosphate mono- and di-anions.

[9] This would be an interesting simulation model for water in the presence of the sodium salts of $ClO_4^-$, $I^-$, $Br^-$, $Cl^-$, $F^-$, $HPO_4^{2-}$, and $SO_4^{2-}$ at various concentrations.

Table 4
Some physical properties of the Hofmeister series of anions

| Effect on proteins, DNA duplexes and triplexes | Anion | van der Waals Surface area $(A_{vdw})$ (Å$^2$)[a] | Effective surface charge Density $\times 10^{-21}$ [$Z^2 \times$ (charge of electron $/A_{vdw}$)][b] (C/Å$^2$) |
|---|---|---|---|
| Decreasing stability | Monovalent | | |
| | $ClO_4^-$ | 81.20 | $-1.97$ |
| | $I^-$ | 55.42 | $-2.89$ |
| | $Br^-$ | 47.78 | $-3.35$ |
| | $Cl^{-\,c}$ | 39.37 | $-4.07$ |
| | $F^{-\,d}$ | 21.24 | $-7.54$ |
| | Divalent | | |
| Increasing stability | $HPO_4^{2-}$ | 88.31 | $-7.26$ |
| | $SO_4^{2-}$ | 82.57 | $-7.76$ |

[a] Calculated using HyperChem 4.0, Hypercube Corp., Gainesville, FL.

[b] Using the expression $Z^2 \times$ (charge of electron$/A_{vdw}$), we observe this newly defined effective surface charge density to correlate with the Hofmeister anion effect. Note that the expressions for ionic strength, $\Gamma/2 = \frac{1}{2} \times$ concentration $\times Z^2$, also scales as $Z^2$, and results from using a Boltzmann distribution to describe the charge distribution in solution.

[c] We expect anions with effective surface charge densities less negative than that of $Cl^-$ to be chaotropes and those with greater negative effective surface charge densities to be kosmotropes.

[d] Since developing the simple physical parameter of effective surface charge density, we have become aware of the work of Jelesarov [28] showing significantly enhanced peptide stability in the presence of high concentrations of $F^-$ and $SO_4^{2-}$.

Table 5
Stabilization of deoxyoligonucleotide triplexes by anions

| 2 M Anion pH 7.0 | $d(T)_{21} \bullet d(A)_{21} \bullet d(T)_{21}$ $T_m$ (°C) | $d(C^+\text{-}T)_6 \bullet d(A\text{-}G)_6 \bullet d(C\text{-}T)_6$ $T_m$ (°C) |
|---|---|---|
| $NaClO_4$ | 44 | – |
| NaCl | 66 | 7 |
| $NaOOCCH_3$ | 66 | 15 |
| $NH_4Cl^*$ | 71 | – |
| $Na_2HPO_4$ | 80 | 15 |
| $Na_2SO_4$ | 80 | 21 |
| $(NH_4)_2\,SO_4{}^*$ | 83 | 28 |

[*] In these salts the cation is $NH_4^+$ instead of $Na^+$; the rank order of their anions is, therefore, not strictly comparable, particularly as $NH_4^+$ enhances nucleic acid helix stability somewhat more than $Na^+$ (see Section 4.3).

the protonation of *C* residues at pH 7.0, so far above their intrinsic p$K_a$ value [3]. It is possible that this difference in $dT_m/d$ log[anion] also includes a contribution from the difference in length between these two triplexes.

In sum, the results of the present work show that water structure-making anions preferentially enhance triplex over duplex stability.

## Acknowledgments

# References

[1] R.D. Blake, J. Massoulié, J.R. Fresco, A spectral approach to the equilibria between polyriboadenylate and polyribouridylate and their complexes, J. Mol. Biol. 30 (1967) 291–308.

[2] K.J. Hampel, P. Crosson, J.S. Lee, Polyamines favor DNA triplex formation at neutral pH, Biochemistry 30 (1991) 4455–4459.

[3] L. Lavelle, J.R. Fresco, UV spectroscopic identification and thermodynamic analysis of protonated third strand deoxycytidine residues at neutrality in the triplex $d(C^+$-$T)_6$:$d(A$-$G)_6$•$d(C$-$T)_6$; evidence for a proton switch, Nucl. Acids Res. 23 (1995) 2692–2705.

[4] R.D. Blake, J.R. Fresco, A spectrophotometric study of the kinetics of formation of the two-stranded helical complex resulting from the interaction of polyriboadenylate and polyribouridylate, J. Mol. Biol. 19 (1996) 145–160.

[5] K.H. Johnson, D.M. Gray, J.C. Sutherland, Vacuum UV CD spectra of homopolymer duplexes and triplexes containing A•T or A•U base pairs, Nucl. Acids Res. 19 (1991) 2275–2280.

[6] J. Wyman, Heme proteins, Adv. Protein Chem. 4 (1948) 407–531.

[7] J. Wyman, Linked function and reciprocal effect in hemoglobin—A second look, Adv. Protein Chem. 19 (1964) 223–286.

[8] J. Wyman, S.J. Gill, Binding and Linkage, Functional Chemistry of Biological Macromolecules, University Science Books, Mill Valley, CA, 1990.

[9] T.M. Record, Analysis of the effect of salts and uncharged solutes on protein and nucleic acid equilibria and processes: a practical guide to recognizing and interpreting polyelectrolyte effects, Hofmeister effects and osmotic effects of salts, Adv. Protein Chem. 51 (1998) 281–353.

[10] S.N. Timasheff, Control of protein stability and reaction by weakly interacting cosolvents, the simplicity of the complicated, Adv. Protein Chem. 51 (1998) 355–432.

[11] C.H. Spink, J.B. Chaires, Effects of hydration, ion release and excluded volume on the melting of triplex and duplex DNA, Biochemistry 38 (1999) 496–508.

[12] D. Matulis, I. Rouzina, V.A. Bloomfield, Thermodynamics of DNA binding and condensation: Isothermal titration calorimetry and electrostatic mechanism, J. Mol. Biol. 296 (2000) 1053–1063.

[13] E.C.W. Clarke, D.N. Glew, Evaluation of the thermodynamic functions for aqueous sodium chloride from equilibrium and calorimetric measurements below 154 °C, J. Phys. Chem. Ref. Data 14 (1985) 489–610.

[14] G.S. Manning, Limiting laws and counterion condensation in polyelectrolyte solutions. 1. Colligative properties, J. Chem. Phys. 51 (1969) 924–933.

[15] G.S. Manning, On the application of polyelectrolyte 'limiting laws' to the helix-coil transition of DNA. I. Excess univalent cations, Biopolymers 11 (1972) 937–949.

[16] G. Manning, J. Roy, Counterion condensation revisited, J. Biomol. Struct. Dyn. 16 (1998) 461–476.

[17] R.A. Robinson, R.H. Stocks, Electrolyte Solutions, Butterworths Scientific Publications, London, 1995, pp. 19, 212, 461, 463, 465, 477.

[18] C.P. Smyth, Dielectric Behavior and Structure, McGraw-Hill, New York, NY, 1955, p. 93.

[19] E.S. Courtenay, M.W. Capp, C.F. Anderson, M.T. Record, Vapor pressure osmometry studies of osmolyte-protein interactions: implications for the action of osmoprotectants in vivo and for the interpretation of 'osmotic stress' experiments in vitro, Biochemistry 39 (2000) 4455–4471.

[20] G. Xie, S.N. Timasheff, The thermodynamic mechanism of protein stabilization by trehalose, Biophys. Chem. 64 (1997) 25–43.

[21] D.C. Rau, V.A. Parsegian, Direct measurement of temperature-dependent solvation forces between DNA double helices, Biophys. J. 61 (1992) 260–271.

[22] (a) F.J. Millero, in: R.A. Horne (Ed.), Water and Aqueous Solutions, Wiley-Interscience, NY, 1972, pp. 519–595
(b) F.J. Millero, in: R.A. Horne (Ed.), Water and Aqueous Solutions, Wiley-Interscience, NY, 1972, pp. 543–560, and references therein.

[23] K.D. Collins, M.W. Washabaugh, The Hofmeister effect and the behaviour of water at interfaces, Quart. Rev. Biophys. 18 (1985) 323–422.

[24] L. Endom, H.G. Hertz, B. Thul, M.D. Zeidler, A microdynamic model of electrolyte solutions as derived from nuclear magnetic relaxation and self-defusion data, Deutsche Bunsenges Phys. Chem. 71 (1967) 1008–1031.

[25] F. Hofmeister, Naunym-Schneidebergs, Archiv für Experimentelle Pathologie Pharmacologie (Leipzig) 24 (1888) 247–260, (For English translation of this paper (# 85-20000) contact The National Translations Center, John Crerar Library, University of Chicago, 5730 S. Ellis Avenue, Chicago, IL 60637, USA).

[26] K. Hamaguchi, E.P. Geiduschek, The effect of electrolytes on the stability of the deoxyribonucleate helix, J. Am. Chem. Soc. 84 (1962) 1329–1338.

[27] J.A. Beebe, J.C. Kurz, C.A. Fierke, Magnesium ions are required by *Bacillus subtilis* ribonuclease P RNA for both binding and cleaving precursor tRNA, Biochemistry 35 (1996) 10493–10505.

[28] I. Jelesarov, E. Durr, R.M. Thomas, H.R. Bosshard, Salt effects on hydrophobic interaction and charge screening in the folding of a negatively charged peptide to a

coiled coil (leucine zipper), Biochemistry 37 (1998) 7539–7550.

[29] W.P. Jencks, CRC Handbook of Biochemistry, selected data for Molecular Biology (1970) p. J-190.

[30] J.I. Partanen, P.O. Minkkinen, Redetermination of the second dissociation constant of phosphoric acid and calculation of the pH values of the pH standards based on solutions of dihydrogen and hydrogen phosphate ions at 298.15 K, Acta Chem. Scandinavica 50 (1996) 1081–1086.